Proceedings of the 28th IEEE
EMBS Annual International Conference
New York City, USA, Aug 30-Sept 3, 2006

A Magnetization Mapping Approach for Passive Shim Design in MRI

H. Sánchez, F. Liu, A. Trakic, S. Crozier

Abstract— **A new passive shim design method is presented which is based on a magnetization mapping approach. Well defined regions with similar magnetization values define the optimal number of passive shims, their shape and position. The new design method is applied in a shimming process without prior-axial shim localization; this reduces the possibility of introducing new errors. The new shim design methodology reduces the number of iterations and the quantity of material required to shim a magnet. Only a few iterations (1-5) are required to shim a whole body horizontal bore magnet with a manufacturing error tolerance larger than 0.1 mm and smaller than 0.5 mm. One numerical example is presented.**

I. Introduction

Two of the most important requirements for high definition Magnetic Resonance Imaging (MRI) experiments are the strength and the spatial quality of the static polarizing magnetic field. It is well-known that the combination of superconducting coils with steel/iron is one of the ways to increase the magnetic flux density magnitude in the region of interest (DSV) and at the same time a considerable reduction in the stray field can be obtained [1]. However, at high field this combination presents some physical limitations when a short bore horizontal magnet is desired. In this case it is desirable to locate the steel/iron close to the superconducting coils; however, high peak fields can be induced in the coil due to the magnetization in the iron. At the same time an over-saturation is produced in the iron due to the high magnitude of the magnetizing field (>1.5T) and the material properties are then governed by the B-H curve. This fact reduces the relative permeability (μ_r) value and hence the possibility of producing a strong contribution to the magnetic field within DSV. Taking into account these constraints, the problem faced is to find the optimal coil and steel/iron shapes and positions which together will produce a high and very homogenous magnetic field in the working volume. At the same time low peak fields inside coils, low stray field and minimum coil/iron volume are desired [2].

This general problem statement can be applied for passive shim design. Passive shimming is an iterative process achieved with small pieces of steel/iron conveniently located around the DSV in such way that the field generated by the coil arrangement plus the field produced by the shim reduces the magnetic field inhomogeneities resulting from the introduced error in the magnet manufacturing process [3]. In this case the problem can be stated as to find out the optimal shim size to bring the magnetic field homogeneity within the MRI requirements using a minimum number of iterations.

The methods presented for iron-superconducting magnet/ shim designs have been limited by algorithms developed for a predefined and fixed iron shape [3],[4].

In the case of passive shim designs, two approaches have been presented for magnets with a horizontal bore. The first method is based on the combination of iron pieces (spheres or rods) to generate a particular harmonic [4]. In the second method an array of iron or steel pieces are uniformly located along the horizontal bore magnet. An optimization algorithm is applied to obtain the minimal piece thickness in each location in such way that the magnetic field superposition generated by all sources produces the target field homogeneity [3]. In all of these methods the iron pieces have a predefined and fixed shape.

In this work we present a new approach for passive shim design taking into account the magnetization map induced by the theoretical magnet design. Constraining the magnetization between a maximal and minimal value, clustered regions of iron pieces with the same magnetization magnitude are obtained. The well consolidated region defines the optimal shim shapes, location and size. In the shimming process the magnetization is calculated using an integral method [5] and both linear and non-linear soft iron can be considered. A magnet design from the literature is shimmed using a classical approach and the new approach proposed in this paper. We demonstrate numerically that the new approach reduces the number of iterations, the total shim thickness and the possibility to introduce new errors in the shimming process.

II. Materials and Methods

We assume two domains of magnetic field sources. One domain consists of elemental cylindrical coils and the other one consists of cylindrical iron pieces. Other domains areas such as the DSV, fringed field surface or sub-domains inside the coil or iron domain can be included. For simplicity consider only the first two mentioned domains. Fig. (1)

Manuscript received April 3, 2006. This work was supported by the Australian Research Council. All authors are with the School of Information Technologic and Electrical Engineering, University of Queensland, Australia. H. Sánchez (e-mail: hsanchez@itee.uq.edu.au). F. Liu (e-mail: feng@itee.uq.edu.au). A. Trakic (e-mail: trakic@itee.uq.edu.au). S. Crozier (e-mail: crozier@itee.uq.edu.au)

shows schematically the initial domain and the optimally shaped domain contour.

The total magnetic field strength produced by the iron and the coils is expressed as [5]:

$$\mathbf{H}^{\mathrm{t}} = \mathbf{H}^{\mathrm{s}} + \mathbf{H}^{\mathrm{m}} \tag{1}$$

where $\mathbf{H}^{\mathrm{s}}$ and $\mathbf{H}^{\mathrm{m}}$ are the magnetic field strength arising from the active region (coils) and passive region (iron) respectively.

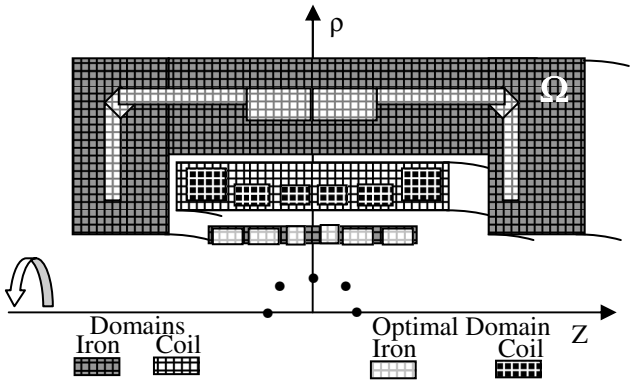

Fig. 1. Schematic representation of the initial domain setup and the final optimal shape for coils and iron. No restrictions are imposed to the initial shape field source domains. Ω represents the iron domain.• target points *p* at DSV ($p = 1\ldots M$); *M* is the number of target points.

The field $\mathbf{H}^{\mathrm{s}}$ can be calculated using The Biot-Savart law in the volume of the current source and the second one can be obtained by a volume integral over the iron domain

$$\mathbf{H}^{\mathrm{m}} = -\frac{1}{4\pi}\nabla_P \int_{\Omega} \mathbf{M}\cdot\nabla_S\left(\frac{1}{\mathrm{R}}\right)d\Omega \tag{2}$$

where R is the distance between the source and the observation point, **M** is the induced magnetization in the iron. In linear magnetic problems $\mathbf{M} = \chi\mathbf{H}$. Assuming the material as isotropic and homogenous then the three vectors **M**, **H** and **B** are collinear.

In order to obtain the total field in DSV using (1), the *priori* knowledge of the induced **M** in the iron by the coil arrangement is required. In order to calculate **M** the iron domain is divided in *N* small iron elements of volume *dV*' where **M** can be assumed uniform throughout *dV*'. Combining (2) and (1), results [5]

$$\begin{pmatrix} \chi s_{i,j}^{\rho\rho} & \chi s_{i,j+\mathrm{N}}^{\rho z} \\ \chi s_{i+\mathrm{N},j}^{z\rho} & \chi s_{i+\mathrm{N},j+\mathrm{N}}^{zz} \end{pmatrix} \begin{pmatrix} H_{\mathrm{z}}^{\mathrm{t}} \\ H_{\rho}^{\mathrm{t}} \end{pmatrix} = \begin{pmatrix} H_{\rho}^{\mathrm{s}} & H_{\mathrm{z}}^{\mathrm{s}} \end{pmatrix} \tag{3}$$

where *N* is the number of iron elements, χ is the iron susceptibility, $H_{\mathrm{z}}^{\mathrm{t}}$ and H_{ρ}^{t} are the axial and radial components of the magnetic field strength in the iron element *i*,

$$s_{im}^{\rho\rho} = \frac{1}{4\pi}\frac{\partial}{\partial\rho}\int_{V'}\frac{\partial}{\partial\rho'}\left(\frac{1}{\mathrm{R}}\right)dV'; s_{im}^{\rho z} = \frac{1}{4\pi}\frac{\partial}{\partial\rho}\int_{V'}\frac{\partial}{\partial z'}\left(\frac{1}{\mathrm{R}}\right)dV'$$

$$s_{im}^{z\rho} = \frac{1}{4\pi}\frac{\partial}{\partial z}\int_{V'}\frac{\partial}{\partial\rho'}\left(\frac{1}{\mathrm{R}}\right)dV'; s_{im}^{zz} = \frac{1}{4\pi}\frac{\partial}{\partial z}\int_{V'}\frac{\partial}{\partial z'}\left(\frac{1}{\mathrm{R}}\right)dV' \tag{4}$$

$dV \sim R_i$, where R_i are the mean radius of each iron element.

Equation (3) can be solved through singular value decomposition, however, we can solve (3) by linear programming (LP) method under linear constraints as follows:

$$\begin{aligned} &\min R\cdot\mathbf{X} \\ &\mathbf{C}*\mathbf{X} \le \mathbf{B}\cdot(1+\varepsilon) \\ &-\mathbf{C}*\mathbf{X} \le -\mathbf{B}\cdot(1-\varepsilon) \\ &H_{\mathrm{z}}^{\mathrm{t}} \le -\mathrm{H}^{\mathrm{z}}{}_{\min}; H_{\mathrm{z}}^{\mathrm{t}} \le \mathrm{H}^{\mathrm{z}}{}_{\max} \\ &H_{\rho}^{\mathrm{t}} \le -\mathrm{H}^{\rho}{}_{\min;} H_{\rho}^{\mathrm{t}} \le \mathrm{H}^{\rho}{}_{\max} \end{aligned} \tag{5}$$

where **X** is the unknown magnetic field strength inside the iron element, **C** is the square matrix containing the interaction among all iron elements, ε is a small relaxing error and ($\mathrm{H}_{\min}^{\rho,z}$, $\mathrm{H}_{\max}^{\rho,z}$) are boundaries that constrain the field strength **H** inside the iron to the useful or target region according with the BH curve, e.g. region of saturation in the case of passive shim design. Problem (5), reduces the iron volume. Due to the boundary constraints in (5), well defined regions of the same magnetization value will be created in the iron domain; those regions define the optimal iron shape for a given coil arrangement. This method in combination with the Current Density Approach [6] provides a complete picture of the coils and iron positions and shapes. This approach will be presented in a future work. In this paper the method is applied for passive shim design.

A. *Passive Shim Design*

In the case of passive shim design, the iron domain is located within and along the horizontal bore of the magnet. See Fig. 1. The iron domain is a cylinder of thickness *T*, ($T << R\mathrm{c}$); *R*c: cylinder radius) and axial length *L*.

To apply the method to shim design, first we must solve (5). If the iron is nonlinear we use the fixed point scheme [5]. Given **M**, the optimal shim shape and by using (2) the magnetic field contribution of each iron piece is calculated at each target point *p* located at the DSV. Equation (2) is proportional to the cross section area Area_i of the iron piece. It means that the shimming problem can be stated as a LP optimization problem with linear constraints [3].

$$\begin{aligned} &\mathrm{Min}\sum_{i=1}^{N}\mathrm{Area}_i \\ &\sum_{i=1}^{N} G_{i,p}\mathrm{Area}_i + B_{\mathrm{z}\,p} - B_{\mathrm{z}}^{\mathrm{m}} \le \frac{T}{2}+\frac{E}{2}; \quad p = 1..M \\ &-\sum_{i=1}^{N} G_{i,p}\mathrm{Area}_i - B_{\mathrm{z}\,p} + B_{\mathrm{z}}^{\mathrm{m}} \le \frac{T}{2}+\frac{E}{2}; \quad p = 1..M. \\ &\mathrm{Area}_i \le \mathrm{Area}_{\max}; \quad i = 1..N \\ &\mathrm{Area}_i \le 0; \qquad i = 1..N; \quad T, B_{\mathrm{z}}^{\mathrm{m}} \ge 0 \end{aligned} \tag{6}$$

The matrix **G** can be determined analytically using (2) or from experiment. The matrix contains the influence of each shim piece *i* at the target or measurement point *p*. B_{zp} is the value of the magnetic field axial component measured at the

target point p prior to the present shimming iteration; B_z^m is the mean value between the maximum and minimum field at DSV. E is the target peak-peak field homogeneity. T is target homogeneity that corresponds to the current iteration. The experimental shimming using (6) have been well described [3].

B. Computational Shimming Simulation.

We assume that we have an arrangement of coils that generates a homogenous magnetic field at DSV. Let E be the peak-peak magnetic field homogeneity at DSV. Within the magnet bore, an iron domain composed by small iron pieces uniformly distributed along the axial and the azimuthally direction, is located. The first step is to find the magnetization in each shim that in combination with the coil arrangement produces the target field homogeneity E. Of course, if no errors are introduced in the coil dimension and position, and the target homogeneity coincides with the E value, then the magnetization or the shim area will be close to zero. To avoid this problem we choose a larger target DSV or smaller E value. We select a larger target DSV since any introduced error in the magnet will be amplified at this new DSV. Under this assumption we assume that each magnet has an optimal shim shape and position capable of reducing E to any field inhomogeneity error larger than E.

Given the magnetization map, the optimal shape and shim positions are determined. In order to simulate the manufacturing errors, uniform random values in the range of the machine tolerances are introduced in all coil blocks. In this paper only errors along the radial and axial dimension were introduced.

The second step is to solve (6) iteratively until the target field homogeneity is reached. If in the first iteration T is set to zero, the problem does not converge and the LP algorithm tends to produce negative areas. To avoid this situation a sequential algorithm is applied to obtain the minimum T value for the current iteration, in which the LP algorithm converges and does not generates negative areas. Then the variable Area_i is updated in all shim locations and a new magnetic field measurement is carried out at the target point p. The new magnetic field measurement contains the field contribution of each updated iron shim solving (3) and using (2). The shimming process is repeated until T =0 ppm. Different from other methods [3], note that the axial shim re-localization step has been avoided in order to reduce the possibility of introducing new errors.

III. Results and Discussions

We have applied the method for the magnet profile presented in reference [7]. A set of passive shims have been generated and a computational simulation of the shimming process has been carried out. Two approaches have been tested: the classical one; shim of the same size uniformly distributed within and along the magnet bore and the new approach described in this paper; optimal shim shape generated with the magnetization map approach.

The magnet generates a magnetic field homogeneity of 10 ppm (E=10 ppm) ppm peak-peak in 45x54 cm DSV. See Fig. 2. The axial length of the cylindrical iron shell was set to 0.6035 m, the radius was set to 0.4271 m. We assume a linear iron with χ= 500.

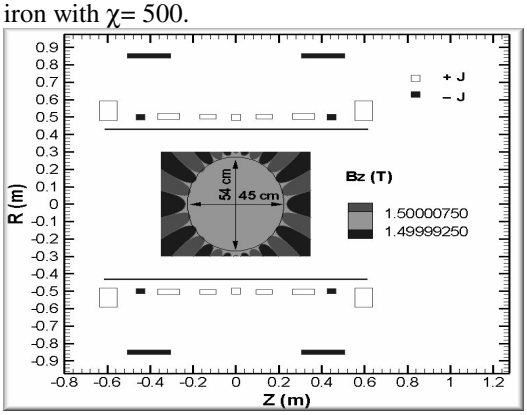

Fig. 2. Cross section of the magnet presented in reference [7]. The continue line located axially along the magnet's bore represents the iron shell.

The magnetization map was obtained for a DSV of 50x60 cm. Note in Fig. 3, the well defined regions of same magnetization values. Due to the azimuthal symmetry the regions of cluster forms ribbons of different axial lengths. In a future work, tesseral errors will be treated.

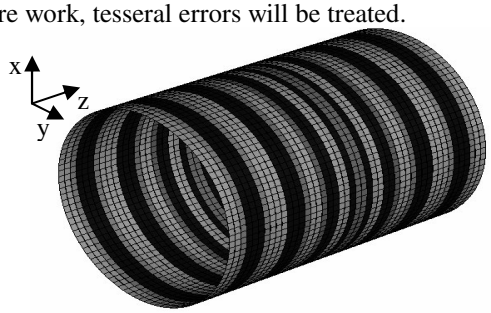

Fig. 3. Representation of the magnetized iron domain.

Appling a filter for values under a threshold, a clear axial gap will appear between the ribbons of iron defining the shim number, shape and position. For this particular case 14 and 16 shims are located along the axial and azimuthal direction, respectively. If the coils are manufactured with a tolerance of 0.5 mm, it means that the random error introduced will be in the range between (-0.5 mm, 0.5 mm). If all coil blocks are perturbed (size and position) along the radial and axial direction then a magnetic field homogeneity around 1000 ppm in the target DSV is generated. See fig.4 (**a**). In order to bring this field homogeneity to the E target value, 4.5 iterations are needed. Minimum reachable field homogeneity of 9.9 ppm is achieved in 10 iterations. Fig. 4 (**b**), shows the shimmed magnetic field homogeneity. Fig. 4(**c**), shows the corresponding shim thicknesses for each axial position. Fig. 4 (**d**), shows the achieved field homogeneity for each iteration. Fig. 5, shows the final shim profile after shimming the magnet.

In order to compare the new shim profiles with the classical shim design [3], four shimming processes were carried out for a given tolerance error.

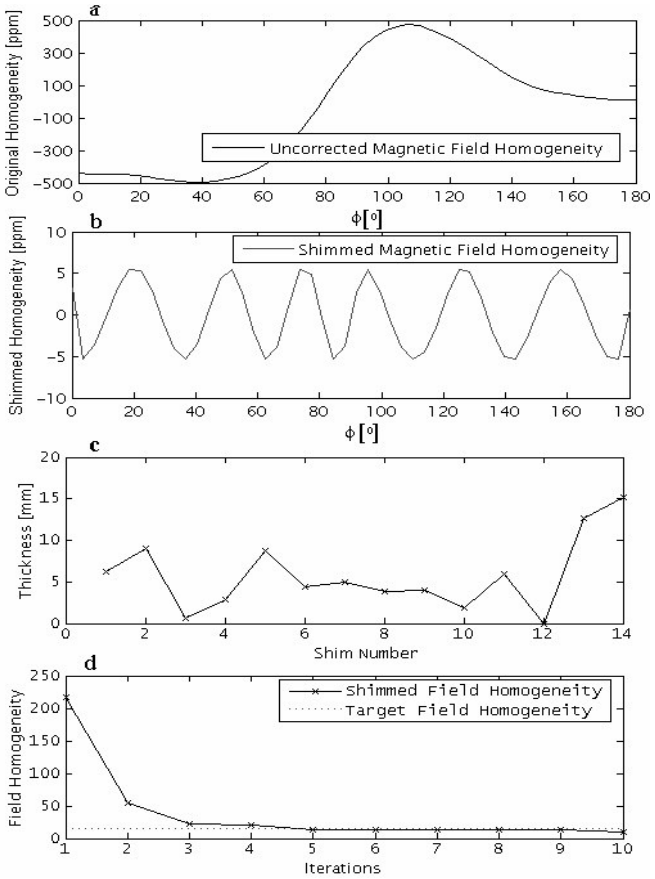

Fig. 4. Original field homogeneity generated by the magnet when errors are introduced (**a**). Field homogeneity profile after the shimming process (**b**). The corresponding thickness for each shim (**c**). The dashed red line shows the target field homogeneity (**d**).

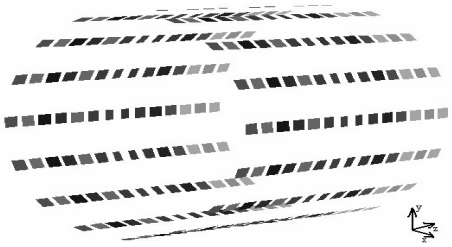

Fig. 5. Final shim profile. Light grays mean larger shim thickness. Note the different shim axial length according to the magnetization map.

Both approaches were evaluated for the same random numbers generated between the given tolerance range. Fig. 6 (**a**), shows that to achieve the target field homogeneity the new approach needs at least 1.4 times less iteration than the classical approach.

The number of iterations can be reduced by locating the shim at the optimal axial position; however, we have avoided this step in order to reduce the possibility of introducing new errors. Note that fewer iterations are needed for real tolerance errors (smaller than 0.5 mm). Fig. 6 (**b**), shows that the maximal shim thickness is required for larger tolerance error. From the curve, we can realize that applying our shim design method, the optimized shim set requires 1.3 times less material than the shim designed using the classical method. It is interesting to note in Fig. 6 (**b**) that for some tolerance errors less material is needed than for smaller tolerance error. This effect is related to the stochastic nature of the introduced error. Some error combinations can produce magnetic field compensation, and hence better field homogeneity than other combinations.

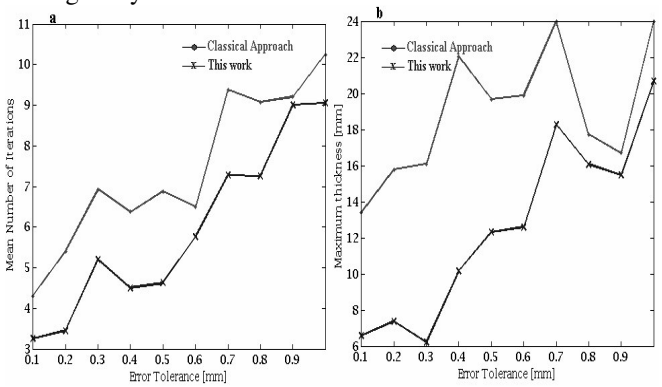

Fig.6. Mean number of iteration needed for a given tolerance error (**a**). Maximum thickness obtained in the four shimming process for a given tolerance error (**b**).

Applying our approach, we can compare the solution stability for different magnets configurations. This new measure can be included as a new parameter in the figure of merit for MRI magnets.

IV. Conclusions

Using the magnetization mapping approach a new shim design method has been presented. Optimal shim shapes and positions are obtained from the well defined cluster of magnetization values. The new approach reduces the number of iterations and the quantity of material required for shimming a magnet. The new shim design and shimming approach reduces the possibility of introducing new errors, avoiding the pre-localization of the optimal shim axial positions. The developed methodology can be useful to evaluate the merit and stability of different magnet configurations.

References

[1] H. Zhao, S. Crozier, "A design method for superconducting MRI magnets with ferromagnetic material," *Meas. Sci. Technol.*, vol. 13, pp. 2047-2052, 2002.

[2] Y. Lvovsky and P. Jarvis, "Superconducting Systems for MRI—Present Solutions and New Trends," *IEEE Trans. Appl. Superconduct.*., vol. 15, pp. 1317-1325, June, 2005.

[3] B. Dorri, V. E. Vermilyea, "Passive Shimming of MR Magnets: algorithm, hardware and results," *IEEE Trans. Mag*., vol 3, pp. 254-257, March, 1993.

[4] C.N. Chen and D.I. Hoult, Biomedical Magnetic Resonance Technology, Adam Hilger, Bristol, 1989.

[5] J. Caldwell, A. Zisserman, R. Saunders, "A GFUN approach to include the effects of iron on coil systems with cylindrical symmetric," *J. Phys. D:Appl. Physc.,* vol 17, pp.1759-1772, 1984.

[6] S. Crozier, H. Zhao, D. M. Doddrell, "Current Density Mapping Approach for Design of Clinical Magnetic Resonance Imaging Magnets," *Concepts Magn Reson*, vol. 15, pp.208-215, 2002.

[7] Y. N. Cheng, T. P. Eagan, R. W. Brown, S. M. Shvartsman, M. R. Thompson, "Design of actively shielded main magnets: an improved functional method," *MAGMA*, vol.16, pp.57–67, 2003.